Quadrupole Moment of the 11^- Intruder Isomer in ^{196}Pb and Its Implications for the 16^- Shears Band Head

K. Vyvey,[1] S. Chmel,[2] G. Neyens,[1] H. Hübel,[2] D. L. Balabanski,[1,3] D. Borremans,[1] N. Coulier,[1] R. Coussement,[1] G. Georgiev,[1] N. Nenoff,[2] S. Pancholi,[4] D. Rossbach,[2] R. Schwengner,[5] S. Teughels,[1] and S. Frauendorf[5,6]

[1]*Instituut voor Kern- en Stralingsfysica, University of Leuven, Celestijnenlaan 200 D, B-3001 Leuven, Belgium*
[2]*Institut für Strahlen- und Kernphysik, Universität Bonn, Nussallee 14-16, D-53115 Bonn, Germany*
[3]*Faculty of Physics, St. Kliment Ohridsky University of Sofia, BG-1164 Sofia, Bulgaria*
[4]*Department of Physics and Astrophysics, Delhi University, Delhi–110007, India*
[5]*Institut für Kern- und Hadronenphysik, Forschungszentrum Rossendorf, PB 510119, D-01314 Dresden, Germany*
[6]*Department of Physics, University of Notre Dame, Notre Dame, Indiana 46556*

(Received 31 October 2001; published 26 February 2002)

The quadrupole moment of the 11^- isomer in ^{196}Pb has been measured by the level mixing spectroscopy method. This state has a $\pi(3s_{1/2}^{-2}1h_{9/2}1i_{13/2})11^-$ configuration which is involved in most of the shears band heads in the Pb region. The first directly measured value of $Q_s(11^-) = (-)3.41(66)$ b, coupled to the previously known quadrupole moment of the $\nu(1i_{13/2}^{-2})12^+$ isomer allows us to estimate the quadrupole moment of the 16^- shears band head as $Q_s(16^-) = -0.32(10)$ b. The experimental values are compared to tilted axis cranking calculations, giving insight into the validity of the additivity approach to couple quadrupole moments and on the amount of deformation in the shears bands.

DOI: 10.1103/PhysRevLett.88.102502 PACS numbers: 21.10.Ky, 21.60.Ev, 23.20.En, 27.80.+w

The discovery of long regular cascades of magnetic dipole ($M1$) transitions in the light Pb and Bi isotopes [1–3], and also in nuclei around mass numbers $A = 80$ [4], 110 [5,6], and 140 [7], led to an extension of the concept of rotation in quantal systems. The $M1$ sequences follow the rotational $I(I + 1)$ behavior, typical for well-deformed nuclei, while lifetime measurements and the weak $E2$ crossover transitions suggest that the nuclear states in these bands are only weakly deformed ($|\beta_2| \leq 0.1$) [8–11]. This contradicts the conventional concept that regular rotational bands exist only in well-deformed nuclei.

The $M1$ bands are built on high-j proton-particle excitations coupled to high-j neutron-hole excitations (or vice versa) [12,13]. The combination of particles and holes energetically favors a perpendicular coupling of their spins, $\vec{j}_\pi$ and $\vec{j}_\nu$, to the total spin $\vec{J}$. Consequently, a large component of the magnetic dipole moment perpendicular to the total spin $\vec{J}$ exists, specifying an orientation in space. The magnetic dipole vector rotates around $\vec{J}$, generating the strong $M1$ radiation. Hence, not an asymmetric charge distribution (as in the case of deformed nuclei), but an asymmetric current distribution allows for the nuclear rotation. This new type of quantal rotation is called "magnetic rotation" to distinguish it from the well-known "electric rotation" of deformed nuclei [14,15]. Along the bands the angular momentum is increased by a step-by-step alignment of the proton and the neutron spins. Since this resembles the closing of a pair of shears, the $M1$ bands are referred to as "shears bands" [13].

In the Pb region the shears bands are based on proton-particle excitations across the $Z = 82$ shell gap coupled to neutron holes in the $1i_{13/2}$ subshell. Typical band-head configurations are, e.g., the $\{\pi(3s_{1/2}^{-2}1h_{9/2}1i_{13/2})_{11^-} \otimes \nu 1i_{13/2}^{-1}\}29/2^-$ state in ^{193}Pb [16,17] and the $\{\pi(3s_{1/2}^{-2}1h_{9/2}1i_{13/2})_{11^-} \otimes \nu(1i_{13/2}^{-2})_{12^+}\}16^-$ state in ^{196}Pb [18,19]. The configuration of the $29/2^-$ isomer in ^{193}Pb has been confirmed unambiguously by a g-factor measurement [17].

In contrast to conventional rotation of deformed nuclei, magnetic rotation occurs in nearly spherical nuclei. However, to date, the deformation has not been measured very accurately. Both static and transition quadrupole moments can provide information on the deformation in the bands. Indeed, the small $E2$ transition probabilities indicate a small deformation. However, an accurate determination of the transition quadrupole moments from lifetime measurements and intensity branching ratios is difficult, because the $E2$ crossover transitions are extremely weak as compared to the strong $M1$ transitions and in many cases they are even below the detection limit. Furthermore, systematic errors introduced through the treatment of the stopping powers in the Doppler-shift attenuation-method experiments might be present [8]. On the other hand, also the direct measurement of the spectroscopic quadrupole moment of the band heads is not straightforward due to their short lifetimes.

This difficulty forces us to take an indirect approach. It is possible to measure the spectroscopic quadrupole moments of the long-lived states which couple to the configurations of the shears bands. The $\pi(3s_{1/2}^{-2}1h_{9/2}1i_{13/2})11^-$ isomer in ^{196}Pb, which has the same proton configuration as the $\{\pi(3s_{1/2}^{-2}1h_{9/2}1i_{13/2})_{11^-} \otimes \nu(1i_{13/2}^{-2})_{12^+}\}16^-$ shears band head in this nucleus [18,19], is determined in this work. The quadrupole moment of the $\nu(1i_{13/2}^{-2})12^+$ isomer, which has the same neutron configuration as the 16^- state, has been measured previously [20]. These two quadrupole moments will be used to constrain the parameters of the theoretical description of the shears bands. We use two approaches: one based on the assumption of the additivity of the quadrupole moments, and another based on the tilted axis cranking (TAC) model [12–15], which has been very successful in describing the properties in the shears bands. A comparison of the results of the two approaches provides evidence for strong nonlinear polarization effects.

The quadrupole moment of the 11^- isomer [$T_{1/2}$ = 72(4) ns] in ^{196}Pb has been measured using the level mixing spectroscopy (LEMS) method [21]. The experiments were performed at the CYCLONE cyclotron in Louvain-la-Neuve. The $^{196}\mathrm{Pb}(I^\pi = 11^-)$ isomer was populated in the $^{\mathrm{nat}}\mathrm{Re}(^{14}\mathrm{N}, 5n)$ reaction at 87 MeV. The 50-μm-thick Re foil served as target, LEMS host, and beam stopper at the same time. A typical in-beam γ-ray spectrum is shown in Fig. 1. The LEMS technique [21] can be understood as follows: After population and alignment of the excited nuclear states in a fusion-evaporation reaction the isomer of interest is embedded in a suitable host where it is exposed to a combined electric quadrupole and magnetic dipole interaction. The electric field gradient (EFG) is provided by the host, which may be either a single crystal or a polycrystal. A split-coil 4.4 T superconducting magnet provides the magnetic field which is oriented parallel to the beam axis, i.e., along the spin-alignment axis. The anisotropy of the γ radiation is measured as a function of the magnetic field strength using four Ge detectors positioned at 0° and 90° with respect to the beam axis. At zero magnetic field only the electric quadrupole interaction is present, caused by the interaction between the nuclear quadrupole moment and the lattice EFG. Because of the misalignment of the EFG with respect to the beam axis the electric quadrupole interaction causes a change of the initial spin alignment. As a consequence, a reduction of the anisotropy of the γ radiation is measured. At high magnetic fields (several Tesla) the electric quadrupole interaction is negligible compared to the magnetic dipole interaction. The spins perform a Larmor precession around the magnetic field. As the precession axis coincides with the spin-alignment axis the initial anisotropy is preserved. At intermediate fields both interactions compete and a smooth change from the hard-core anisotropy to the initial full anisotropy is observed. This part of the LEMS curve is sensitive to the ratio ν_Q/ν_μ of the quadrupole interaction frequency, $\nu_Q = eQV_{ZZ}/h$, to the magnetic interaction frequency, $\nu_\mu = \mu B/h$, where μ is the magnetic moment of the isomer. If the magnetic moment μ and the electric field gradient V_{ZZ} are known a value for the quadrupole moment can be extracted [21,22].

As Re has a hexagonal close-packed lattice structure [23] it is a good candidate for a LEMS host. In our experiment, which was performed at room temperature, the EFG could be calibrated by using the known quadrupole moment of the $I^\pi = 12^+$ [$T_{1/2}$ = 269(5) ns, $\mu = -1.920(18)\mu_N$, $Q_s = 0.65(5)e$ b] isomer in ^{196}Pb [20,24]. A partial level scheme [25] is shown in Fig. 2. Figure 3a shows the LEMS curve obtained for the 337 keV ($E1, 10^+ \to 9^-$) transition mainly fed via the 12^+ isomer (82%) [25]. The fit, using the measured magnetic moment, results in a quadrupole interaction frequency of ν_Q = 38(3) MHz. This result includes a correction for the 10% feeding of the 10^+ state via the $11^- \to 12^+$ cascade and the 5% feeding of the 10^+ state directly from the 11^- isomer [26]. The different detector combinations gave a

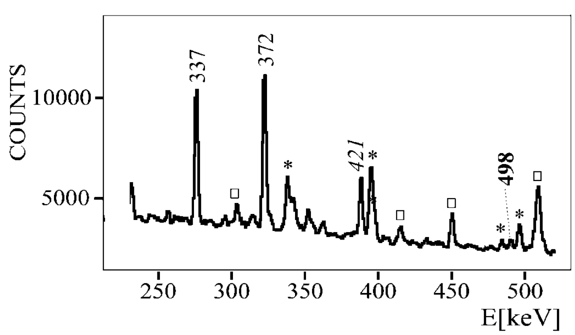

FIG. 1. A typical γ-ray spectrum, without time gate, obtained in the $^{\mathrm{nat}}\mathrm{Re}(^{14}\mathrm{N}, xn)$ reaction at 87 MeV. The peaks coming from the 12^+ and the 11^- isomers are indicated in a normal and bold font, respectively. Contaminating radiation, which is either prompt or from other isomers or β decay, is marked with a square, a cross, and an asterisk, respectively.

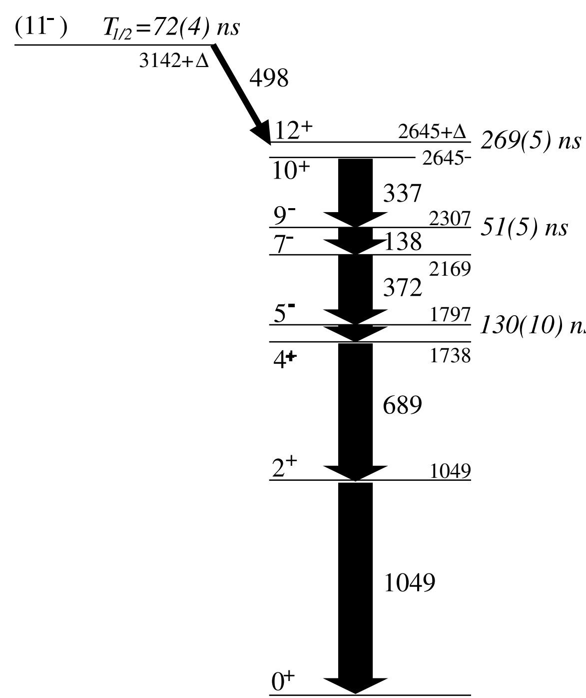

FIG. 2. Partial level scheme of the ^{196}Pb nucleus (taken from Ref. [25]. The thicknesses of the arrows is proportional to the γ ray intensities.

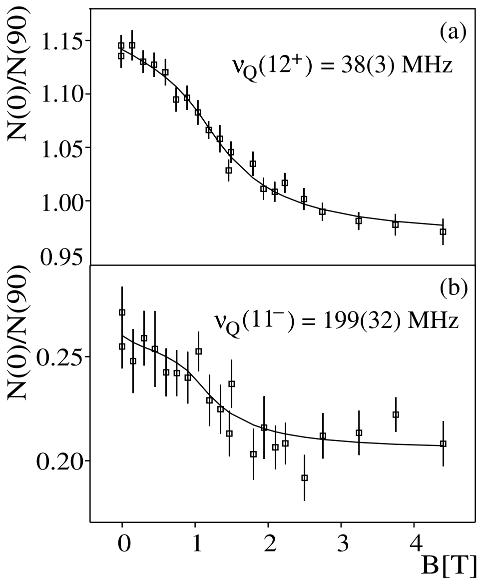

FIG. 3. (a) LEMS curve obtained for the 337 ($E1, 10^+ \rightarrow 9^-$) keV transition. (b) LEMS curve obtained for the 498 ($E1, 11^- \rightarrow 12^+$) keV transition.

consistent result for the quadrupole interaction frequency ν_Q and the average value has been adopted. The spread in the quadrupole frequencies obtained by the different fits lies within the limits of the quoted experimental uncertainty. Using the known quadrupole moment an EFG of $|V_{ZZ}(\mathrm{Pb}\underline{\mathrm{Re}})| = 2.42(27) \cdot 10^{21}$ V/m^2 is deduced.

Figure 3b shows the LEMS curve obtained for the 498 keV $E1$ transition depopulating the 11^- isomer [25]. The fit, making use of the experimental magnetic moment $\mu(11^-) = 10.56(88)\mu_N$ [27], results in a quadrupole interaction frequency of $\nu_Q = 199(32)$ MHz. The analysis was performed in a similar way as for the 12^+ isomer. The quoted uncertainties include the uncertainties on the corresponding magnetic moments as well. From the ratio $\nu_Q(11^-)/\nu_Q(12^+)$ a value of $Q_s(11^-) = (-)3.41(66)$ b is extracted. Note that LEMS measurements are not sensitive to the sign of the quadrupole moment. The negative sign is adopted because the 11^- isomer can be considered as a slightly oblate ^{194}Hg core with two valence protons in nearly parallel orbitals around its symmetry axis. In order to maximize the overlap of the wave functions of the valence particles and the nuclear core, the nucleus will take an oblate deformation.

Assuming that the 11^- and 12^+ isomers are axially symmetric deformed homogeneous charge distributions with their spins aligned along their respective deformation axes (i.e., K is a good quantum number and $K = I$) we may use the formulas [28] $Q_s = Q_0 \frac{3K^2 - I(I+1)}{(I+1)(2I+1)}$ and $Q_0 = \frac{3}{\sqrt{5\pi}} R_0^2 Z \beta_2 (1 + 0.36\beta_2)$ to obtain the intrinsic quadrupole moments $Q_0(11^-) = -4.43(85)$ b and $Q_0(12^+) = 0.82(6)$ b and the deformation parameters $\beta_2(11^-) = -0.156(28)$ and $\beta_2(12^+) = 0.027(2)$ for the 11^- proton and 12^+ neutron states, respectively.

These experimental quadrupole moments will now be used as input for the two models applied for estimating the quadrupole moment of the 16^- band head. First, we assume the additivity of the E_2^0 quadrupole operator, $E_2^0(\mathrm{tot}) = E_2^0(\pi) + E_2^0(\nu)$. This seems to be a reasonable approach because it is experimentally proven that the additivity works well to couple the magnetic moments of the proton and the neutron configuration to that of the shears band head [17]. Possible admixtures in the wave functions of the 11^- and the 12^+ isomers are automatically taken into account by using the measured quadrupole moments. Applying the angular momentum coupling rules and tensor algebra [29], we then obtain the spectroscopic quadrupole moment of the band head

$$\begin{aligned} Q_s(16^-) &= \sqrt{\frac{16\pi}{5}} \langle 16, 16 \,|\, E_2^0(\mathrm{tot}) \,|\, 16, 16 \rangle \\ &= -0.32(10) \text{ b}. \end{aligned} \tag{1}$$

Second, the quadrupole moments have been calculated using the TAC model based on the pairing plus quadrupole-quadrupole interaction. We use the model as described in Ref. [30], except that the electric quadrupole moment is calculated as the expectation value of the proton system. The crucial parameter of the model is the quadrupole-quadrupole coupling constant, κ, which controls the size of the deformation. We adjust that parameter such that the experimental quadrupole moment of the $\nu(1i_{13/2}^{-2})12^+$ isomer, $Q_s(12^+) = 0.65$ b [20], is reproduced. With this value for κ, which is 8% larger than the previously used value, we obtain $Q_s^{\mathrm{TAC}}(11^-) = -2.86$ b for the $(\pi 3s_{1/2}^{-2} 1h_{9/2} 1i_{13/2})11^-$ configuration. The corresponding calculated deformations are $\beta_2^{\mathrm{TAC}}(11^-) = -0.127$ and $\beta_2^{\mathrm{TAC}}(12^+) = 0.044$, respectively. Thus, both the experimental and the theoretical results suggest that the 11^- isomer is moderately deformed. This is in agreement with former calculations, making use of the Woods-Saxon potential, the monopole pairing interaction, the standard Strutinsky renormalization, and the Lipkin-Nogami treatment of the pairing problem. They result in similar values for the first excited $0^+(\pi[505\ 9/2])^2$ state and the $11^-(\pi[505\ 9/2]\pi[606\ 13/2])$ configuration in ^{196}Pb: $\beta_2 \approx -0.17$ [31].

The same parameter set can now be used to calculate the quadrupole moment and the deformation of the 16^- shears band head. This results in $Q_s^{\mathrm{TAC}}(16^-) = -1.2$ b and $\beta_2^{\mathrm{TAC}}(16^-) = -0.134$, respectively. Hence, the TAC model predicts that the deformation of the shears band head is similar to the deformation of the 11^- intruder isomer. The obtained deformation suggests that the $M1$ band built on the 16^- state might be not only due to a rotating magnetic dipole vector, but also in part due to rotation of the weakly deformed charge distribution.

The 16^- quadrupole moment as deduced from additive coupling of the experimental $Q_{\rm exp}(11^-)$ and $Q_{\rm exp}(12^+)$ is almost four times smaller than the one calculated by the TAC model. The additivity approach assumes that the quadrupole polarization of the core induced by the valence protons does not change the polarization induced by the valence neutrons. However, such an approach does not take into account the additional proton-neutron correlations between the high-j valence nucleons in the 16^- state. It is well known that the strongly attractive interactions between the excited protons and the valence neutrons drive the nucleus towards a more deformed shape [32]. In addition, TAC calculations show that the $3s_{1/2}^{-2}$ proton holes contribute about 50% to the 11^- proton quadrupole moment (through mixing with the $d_{3/2,5/2}$ and $g_{7/2}$ orbitals) and the low-j $p_{1/2,3/2}$ and $f_{5/2}$ neutron holes contribute also about 50% to the 12^+ neutron quadrupole moment. When calculating the quadrupole moment of the 16^- state the interactions between these low-j proton and neutron orbitals must not be neglected. These self-interactions substantially increase the 16^- quadrupole moment, which is no longer proportional to the quadrupole moments of the 11^- and 12^+ states.

The breakdown of additivity reflects the softness of the nucleus with respect to quadrupole deformations. This stresses the importance of measuring quadrupole moments, which are much more sensitive to collective admixtures in the wave functions and, hence, polarization effects than magnetic moments [29,33]. Therefore, the additivity approach is not accurate enough for quadrupole moments, while it is a good approximation for magnetic moments.

In conclusion, we have measured the spectroscopic quadrupole moment of the 11^- isomer in ^{196}Pb, $Q_s(11^-) = (-)3.41(66)$ b, corresponding to a deformation of $\beta_2(11^-) = (-)0.156(28)$. This value and the previously measured quadrupole moment of the $\nu(1i_{13/2}^{-2})12^+$ isomeric state in ^{196}Pb set a narrow constraint on the parameter of the TAC model that controls the deformation. It is possible to reproduce, within the uncertainty limits, both quadrupole moments with one and the same parameter value. While the 12^+ neutron hole state is nearly spherical $[\beta_2^{\rm TAC}(12^+) = 0.044]$ the 11^- state is found to be moderately deformed $[\beta_2^{\rm TAC}(11^-) = -0.127]$. Using the same model parameter as for the 11^- and 12^+ isomers, the TAC model predicts that the 16^- shears band head has a quadrupole moment of $Q_s(16^-) = -1.2$ b which corresponds to a deformation of $\beta_2 = -0.13$. This indicates that the $M1$ bands are, at least near the band head, moderately oblate deformed. Coupling the measured quadrupole moments of the 11^- proton and the 12^+ neutron component of the 16^- band head in an additive way results in a smaller value for the quadrupole moment $[Q_s = -0.32(10)$ b$]$. The strong interaction between the neutron and proton quadrupole moments causes the breakdown of the additivity. A direct measurement of the quadrupole moment of the shears band head is needed to confirm these suggestions.

The authors thank the staff of the CYCLONE cyclotron. This work was partially financed by the IUAP Project No. p4-07 with a grant for G. G., K. V., and G. N. were supported by the FWO-Vlaanderen. D. L. B. acknowledges grants by DWTC-Belgium and NATO. The Bonn group was supported by the Deutsche Forschungsgemeinschaft under Contract No. Hu 325/10. Support through the EU Contract No. ERB FMG ECT 950026 and DOE Grant No. DE-FG02-95ER40934 is also acknowledged.

[1] G. Baldsiefen *et al.,* in *Proceedings of the Xth International School on Nuclear Physics and Nuclear Energy, Varna, Bulgaria, 1991,* edited by W. Andrejtscheff and D. Elekkov (Inst. Nucl. Research Nucl. Energy, Sofia, 1991), p. 10; Phys. Lett. B **275**, 252 (1992).
[2] Amita, A. K. Jain, and B. Singh, At. Data Nucl. Data Tables **74**, 283 (2000).
[3] R. M. Clark and A. O. Macchiavelli, Annu. Rev. Nucl. Part. Sci. **50**, 1 (2000).
[4] H. Schnare *et al.,* Phys. Rev. Lett. **82**, 4408 (1999).
[5] F. Brandolini *et al.,* Phys. Lett. B **388**, 468 (1996).
[6] S. Juutinen *et al.,* Nucl. Phys. **A573**, 306 (1994).
[7] A. Gadea *et al.,* Phys. Rev. C **55**, 1 (1997).
[8] R. M. Clark *et al.,* Phys. Rev. Lett. **78**, 1868 (1997).
[9] R. M. Clark *et al.,* Phys. Lett. B **440**, 251 (1998).
[10] R. Krücken *et al.,* Phys. Rev. C **58**, R1876 (1998).
[11] G. Kemper *et al.,* Eur. Phys. J. **A11**, 121 (2001).
[12] S. Frauendorf, Nucl. Phys. **A557**, 259c (1993).
[13] G. Baldsiefen *et al.,* Nucl. Phys. **A574**, 521 (1994).
[14] S. Frauendorf, Z. Phys. A **358**, 163 (1997).
[15] S. Frauendorf, Rev. Mod. Phys. **73**, 463 (2001).
[16] J. M. Lagrange *et al.,* Nucl. Phys. **A530**, 437 (1991).
[17] S. Chmel *et al.,* Phys. Rev. Lett. **79**, 2002 (1997).
[18] J. R. Hughes *et al.,* Phys. Rev. C **47**, R1337 (1993).
[19] G. Baldsiefen *et al.,* Z. Phys. A **355**, 337 (1996).
[20] S. Zywietz *et al.,* Hyperfine Interact. **9**, 109 (1981).
[21] F. Hardeman *et al.,* Phys. Rev. C **43**, 130 (1991).
[22] F. Hardeman *et al.,* Hyperfine Interact. **59**, 13 (1990).
[23] *Handbook of Chemistry and Physics,* edited by R. C. Weast (CRC Press, Cleveland, 1977).
[24] C. Stenzel *et al.,* Nucl. Phys. **A411**, 248 (1983).
[25] J. J. Van Ruyven *et al.,* Nucl. Phys. **A449**, 579 (1986).
[26] K. Vyvey *et al.,* Phys. Rev. C (to be published).
[27] J. Penninga *et al.,* Nucl. Phys. **A471**, 535 (1987).
[28] K. E. G. Löbner *et al.,* Nucl. Data Tables A **7**, 495 (1970).
[29] K. L. G. Heyde, *The Nuclear Shell Model* (Springer-Verlag, Berlin, 1994), 2nd ed.
[30] S. Frauendorf, Nucl. Phys. **A677**, 115 (2000).
[31] R. Bengtsson *et al.,* Z. Phys. A **334**, 269 (1989).
[32] K. Heyde *et al.,* Nucl. Phys. **A466**, 189 (1987).
[33] K. Heyde, Hyperfine Interact. **75**, 69 (1992).